



## Young's Modulus of Single and Double Walled Carbon Nanocones Using Finite Element Method

M. Mohammadian<sup>a\*</sup>, A. Fereidoon<sup>b</sup>

<sup>a</sup>Department of Mechanical Engineering, University of Islamic Azad, Gorgan branch, Kordkuy center

<sup>b</sup> Faculty of Mechanical Engineering, University of Semnan

### PAPER INFO

#### Paper history:

Received 08 November 2013

Received in revised form 27 February 2014

Accepted 22 May 2014

#### Keywords:

Carbon Nanocones

Truss Model

LINK8 Element

ANSYS

### ABSTRACT

In this paper, a three-dimensional finite element (FE) model of carbon nanocones (CNCs) is proposed and used for obtaining Young's modulus of CNCs. In this model, stretching and bending forces between carbon atoms are simulated using truss elements in ANSYS software. Then, the model is subjected to the tension and by obtaining the stiffness of the CNC and using elasticity theory, Young's modulus is calculated. The results showed that for a fixed length of CNC, the modulus increase with the increase in diameter whereas it decreases by an increase in the apex angle. Also, Young's modulus of double walled carbon nanocones (DWCNCs) obtained between the values of each layer. Furthermore, it is showed that elastic modulus can be effected by defects and their positions in CNC.

doi:10.5829/idosi.ije.2014.27.09c.17

## 1. INTRODUCTION

Carbon nanocones are a group of carbon-based nanostructures which are conical graphitic structures and have unique mechanical, electrical and thermal properties [1-3]. CNCs can be used as probes in scanning tunneling microscope (STM), atomic force microscope (AFM), magnetic force microscopy (MFM), gas sensors, energy storage and biosensors [4-6]. Also, they have potential applications in nanoindentations and electron fieldemitters [7, 8]. For CNCs, five apex angles of 19.2°, 38.9°, 60°, 86.6° and 123.6° are proposed by Ge and Sattler [9]. Due to the application of carbon nanotubes (CNTs) and CNCs in nanocomposites, investigation of elastic modulus will be very useful [10, 11]. Young's modulus is one of the important mechanical properties of the materials.

According to the authors' knowledge, not many research works were found about mechanical and Young's modulus of CNCs in the available literature. Molecular dynamics (MD) simulations are widely used by researches in investigation of mechanical and

thermal properties of CNCs. By this method, Wei et. al. [1] studied the elastic and plastic properties of single-walled carbon nanocones (SWCNCs). Tsai and Fang [12] investigated the thermal stability of the CNC. In addition, MD method is used by Liew et. al. [13] in buckling behavior of CNCs, and is used by Liao et. al. [14] in tensile and compressive behaviors of open-tip CNCs. Kumar et al. [15] investigated the Young's and shear modulus of CNCs by employing second-generation reactive empirical bond-order potential. They found that the value of Young's modulus lies in the range of 0.24 Tpa to 0.73 Tpa, and the Shear modulus varies from 0.1 Tpa to 0.29 Tpa. Also, vibration properties of CNCs are studied by researchers. Abadiet et al. [16] and Fakhrabadi et al. [17] used, respectively, nonlocal continuum shell model and molecular mechanics approach in free vibration analysis of CNCs.

In this paper, a truss model of graphene sheet and CNT is proposed and developed for construction of single walled carbon nanocones (SWCNCs) and DWCNCs. Nearly, similar models are used by researchers in investigation of CNTs. Chang and Gao [18] used an elastic rod and a spiral spring to model the stretching and twisting bonds. Also, similar rod-spring geometric configuration is performed by Nasdala and

\*Corresponding Author Email: [Mo.mohammadyan@gmail.com](mailto:Mo.mohammadyan@gmail.com) (M. Mohammadian)

Ernst [19]. They calculated the properties of the structure by fitting MD and ab initio analysis. Leung et al. [20] have used three rods in the hexagonal unit of carbon atoms. One of them is used in C–C bonds and two others are named as factious trusses and utilized for the non-bonds carbon atoms. Nahaz and Rabou [21] obtained the Young's modulus of graphene sheet and a CNT by similar truss finite element model. Based on non-linear interatomic potentials, Rafiee and Heidarhaei [22] used non-linear spring elements for C-C bonds. Using this model, they studied the Young's modulus of CNTs.

In this paper, two elastic rods are used to represent the bond stretching and angle variation in the hexagonal unit of carbon atoms. There are two differences between the work done in this paper and the works of investigators mentioned. The first difference is the values that are obtained for the characteristics of the rods, and the second is using the model in the CNCs. Our review shows that this model hasn't been used so far in obtaining Young's modulus of CNCs.

This paper contains the following sections: First, the structure and the properties of SWCNCs and multi walled carbon nanocones (MWCNCs) are described. Second, characteristics of the rods in truss model are obtained using potential energy of a molecular system. Third, the model is used by finite element method for calculating Young's modulus of graphene sheet and CNTs and results compared with the findings of other researchers. Finally, Young's modulus of SWCNCs and DWCNCs is obtained by the presented model and effect of defects is discussed.

## 2. THE STRUCTURE OF SWCNCs AND MWCNCs

Graphene sheet can be rolled in a desired direction and then, if the open edges are joined to each other, a SWCNC will be constructed. Carbon nanocones can be produced by chemical vapor deposition (CVD) method and also by using plasma for decomposing hydrocarbons [23, 24]. Because the hexagonal texture of graphene sheet must be maintained, the apex angle of the cone can't be arbitrary angle. There are only five possible apex angles for nanocones which can be obtained as follows [25]:

$$a = 2 \arcsin\left(1 - \frac{q}{360}\right) \quad (1)$$

where,  $\theta$  is the disclination angle in degrees. By selecting the values of  $\theta$  as  $60^\circ$ ,  $120^\circ$ ,  $180^\circ$ ,  $240^\circ$  and  $300^\circ$ , the apex angles of closed cones will be  $112.9^\circ$ ,  $83.6^\circ$ ,  $60^\circ$ ,  $38.9^\circ$  and  $19.2^\circ$ , respectively. It can be seen that CNTs are special cases of CNCs with zero apex angle. For instance, Figure 1 demonstrates the graphene sheet with the disclination angle of  $240^\circ$  and the constructed SWCNC with the apex angle of  $38.9^\circ$ .

Analogous to CNTs, the CNCs can also be found as MWCNCs according to their number of layers.

When some SWCNCs are put on each other with longitudinal distance, they form a multi walled carbon nanocone. The apex angle of each layer can be different with the other layers. In Figure 1, a MWCNC with the same apex angle for all layers is depicted.

## 3. ATOMISTIC MODELING

The atomistic approaches in modeling of CNTs and CNCs are computationally expensive. Thus, in this paper FEM is used by a linkage between inter atomic potential energies of molecular structure and an equivalent structure model. By this method, results of modeling of CNTs and nanocomposites are in good agreement with the results of atomistic approaches [10, 17, 21].

Finite element model of an open-tip CNC with a hexagonal unit of carbon atoms is shown in Figure 2.

Each hexagonal includes two types of elastic rod which are used for representing the interaction forces between carbon atoms. Here, we determine the characteristics of the rods which are needed in FEM.

The total potential energy of a molecular system can be obtained from Equation (2) [18]:

$$U = \sum U_r + \sum U_q + \sum U_j + \sum U_w + \sum U_{vdw} \quad (2)$$

where,  $U_r$ ,  $U_\theta$ ,  $U_\phi$ ,  $U_\omega$  and  $U_{vdw}$  are energies that are related to the bond stretching, angle variation, dihedral, out of plane torsional and van der Waals (vdW), respectively. Dihedral, torsional and vdW energies are ignorable and can be neglected in comparison with the other energies [26]. Therefore, in small strains Equation (2) can be simplified as follow:

$$U = \sum U_r + \sum U_q \quad (3)$$

The two terms of above equation can be formulated as below [20]:

$$U_r = K_r (R - R_0)^2 \quad (4)$$

$$U_q = K_q (q - q_0)^2 \quad (5)$$

where,  $R$ ,  $R_0$ ,  $\theta$  and  $\theta_0$  are the secondary length, initial length, varied angle and initial angle, respectively.  $K_r$  and  $K_\theta$  are force constants which are equal to 326 nN/nm and 0.438 nN.nm, respectively.

In Figure 2, solid and dashed lines are rods with circular cross section and represent stretching and angle variation between bond and non-bond carbon atoms, respectively. Since the rods can't be bended and they can only be stretched, the strain energy ( $U$ ) of a rod will be:

$$U_r = \frac{1}{2} \left( \frac{AE}{L} \right) (\Delta L)^2 \tag{6}$$

where, A, E, L and ΔL are the cross section area, the Young’s modulus, the length and the length variation of the rod, respectively. In Equation (4), the term (R-R<sub>0</sub>)<sup>2</sup> is equal to the term ΔL<sup>2</sup> in Equation (6). Therefore, by comparing Equation (4) and Equation (6), the Young’s modulus of the bond rods are obtained as follows:

$$E_{bond} = \frac{2LK_r}{A} \tag{7}$$

For the non-bond rods, the angle variation (Δθ) must be correlated to the length variation (ΔS). From Figure 2, the relation between L, S and θ is:

$$S^2 = 2L^2(1 - \cos q) \tag{8}$$

The first derivation of above equation is:

$$\frac{dS}{dq} = \frac{L^2 \sin q}{S} \tag{9}$$

By substituting θ=120° in Equation (9), we have dS/dθ=L/2. So, for the small displacements, the relation between Δθ and ΔS will be:

$$\Delta q = \frac{2}{L} \Delta S \tag{10}$$

Hence, by using Equation (5) and Equation (6), the Young’s modulus for the non-bond rods are obtained as follow:

$$E_{non-bond} = \frac{8SK_q}{AL^2} \tag{11}$$

The value of A is obtained from minimization of the total strain energy of the structure. The details of the procedure can be found in [27]. By substituting A=0.0015 nm<sup>2</sup>, L= 0.142 nm and S=0.24595 nm, the Young’s modulus of the rods can be calculated as follow:

$$E_{bond}=61.72\text{Tpa}, E_{non-bond}=28.36\text{Tpa}$$

The above numerical values are fed into the required properties of the rod elements in finite element models.

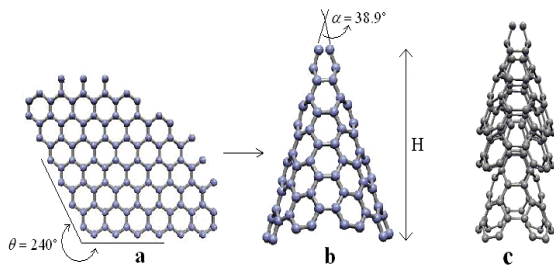


**Figure 1.** a) Graphene sheet with the disclination angle of 240°, b) A CNC with the apex angle of 38.9°, c) A MWCNC

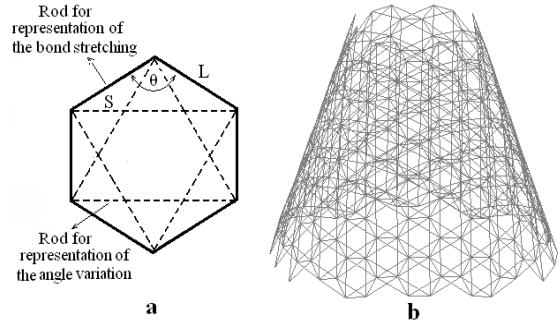


**Figure 2.** a) Hexagonal unit of carbon atoms b) Finite element model of an open- tip CNC

**4. RESULTS AND DISSCUSION**

In this section, using the mentioned model, Young’s modulus of graphene sheet and CNTs are calculated and compared with the results of other investigators. Then, SWCNCs and DWCNCs are modeled and young’s modulus is obtained.

**4. 1. Modeling of Graphene Sheet**

Four different sizes of graphene sheet are modeled using 2D LINK1 elements in ANSYS software. In all cases, the nodes which are located in the left end are fully fixed and the nodes in the right end are subjected to a horizontal stretching of 0.001 nm. This value is selected to avoid nonlinearity of the analysis. The stretching lead to reaction forces in the fully fixed nodes and these forces can be determined by finite element method. By summing the total reaction forces in x direction (F<sub>x</sub>) and having the longitudinal stretching (Δl=0.001 nm), the stiffness (K) of the graphene sheet can be calculated by the following equation:

$$K = \frac{\sum F_x}{\Delta l} \tag{12}$$

Consequently, the Young's modulus is obtained from Equation (13):

$$E = \frac{KL}{A} \tag{13}$$

where, L is the length and A=Wt is the cross section which are of a graphene sheet with width W and thickness t. The thickness is assumed to be equal to interlayer spacing of graphite, 0.34 nm. The Young’s modulus is calculated for graphene sheets by using Equation (13) and presented in Table 1. The results are in good agreement with the findings of Li and Chou [28].

For instance, finite element model of a graphene sheet and generated axial stresses are depicted in Figure 3. The length and the width of the sheet are

approximately 3.13 nm and 0.98 nm, respectively. This model includes 182 nodes and 568 elements. The maximum value of axial stress is obtained about 12.8Gpa.

**4. 2. Modeling of CNT** For investigating the applicability of the proposed model during obtaining Young's modulus of carbon nanotubes, four CNTs with different values of lengths and diameters are modeled using 3D LINK8 elements in ANSYS software. In all cases, one side of the model is fully fixed and the other side is subjected to a longitudinal stretching of 0.001 nm. For example, Figure 4 demonstrates the finite element model and axial stresses for a CNT with the diameter of 1.085 nm and the length of about 2 nm. In this case, the maximum value of axial stress is 14.2Gpa. The reaction forces are obtained by ANSYS data and the stiffness and Young's modulus calculated by Equations (12) and (13). The value of  $A$  in Equation (13) is equal to  $\pi Dt$ , where  $D$  is the mean diameter of the CNT and  $t$  is the thickness which is assumed to be 0.34 nm. The results are presented in Table 2. The average value of Young's modulus is obtained as 0.996Tpa which is very close to 1.042 Tpa that is obtained by researches [28, 29].

**4. 3. Modeling of SWCNC and DWCNC** As be showed before, the presented model in section 3 with the obtained characteristics is suitable in modeling of graphene sheet and CNTs. Thus, this model is used for obtaining the Young's modulus of CNCs. In this paper, due to geometric limitations at the apex of CNC, four open-tip SWCNCs with the apex angle of  $19.2^\circ$  and  $38.9^\circ$  are modeled in ANSYS software using 3DLINK8 elements. These models are named as case 1, case 2, case 3 and case 4. The length of the CNCs is fixed and is approximately  $14\text{\AA}$ . Other geometric dimensions and the number of nodes and elements for the cases are listed in Table 3. By using the SWCNCs which are presented in Table 3, two DWCNCs are constructed. One of them is named as DWCNC1 and is the combination of case 1 and case 2 with the apex angle of  $19.2^\circ$  and the other one is combination of case 3 and case 4 and is named as DWCNC2 with the apex angle of  $38.9^\circ$ . In concentric MWCNCs, Ansari et al. showed that if the longitudinal distance ( $Z$ ) between the cones apex be larger than  $9\text{\AA}$ , the vdW force between the two layers is negligible and can be ignored [25]. So, the dimensions of SWCNCs which are presented in Table 3 are selected so that in constructed DWCNCs, the vdW force is negligible.

The same mechanical and geometrical properties of graphene sheet and CNT are applied for the elements in SWCNCs and DWCNCs. Similar to the boundary condition of CNT and graphene sheet, the CNCs are fully fixed at the side with the largest radius. The other side is subjected to a longitudinal stretching of 0.001nm.

For instance, finite element model and generated axial stresses for SWCNCs and DWCNCs are shown in Figures 5 and 6, respectively.

By substituting  $n=1$  and  $n=2$  in Equation (17) which is described in appendix, the Young's modulus is calculated and presented in Table 4. As it is obvious in this table, the obtained values for the Young's modulus of CNCs are smaller than those of CNTs. In CNTs, this value is about 1.042Tpa whereas for the CNCs the value is obtained in the range of 0.4 Tpa to 0.7 Tpa. As it was reviewed in introduction, Kumar et al. [15] found that the value of Young's modulus for CNCs with different geometrical dimension lies in the range of 0.24 Tpa to 0.73 Tpa. Therefore, the results of presented model for CNCs are in good agreement with the findings of Kumar et al. [15]. By attention in Table 4, it is found that by increasing the apex angle, the Young's modulus decreased. The reason is that by increasing the apex angle in a cone with a specified length, the difference between the largest and smallest radius increases and thus the cone gets away further from the cylindrical shape. Also, by comparing case 1 with case 2 and case 3 with case 4, we found that in a desired apex angle, increasing the smaller radius can lead to increment of Young's modulus. Table 4 shows that values of Young's modulus in DWCNCs are located between the values of each layer. This result is different for the CNTs. In multi-walled carbon nanotubes, Young's modulus is larger than those of each layer and by increasing the layers, elastic constant increase.

**4. 4. Defected Carbon Nanocones** Due to the restrictions of CNT manufacturing, the production of perfect nanotubes is very hard, and the percentage of those is very low compared to the percentage of defect nanotubes. Vacancies result from missing carbon atoms in the CNT walls. This can happen when CNTs are subjected to irradiation [30]. The distribution and types of defects in CNT will play a central role in their mechanical strength [31]. In this section, the FE model is developed to investigate the effect of defect and its position on Young's modulus of CNCs.

For modeling, one carbon atom with bonds and non-bonds elements is omitted from the CNCs. This defect is created in two opposite points and three positions are considered for them. As depicted in Figure 7, two defects are located at two end of CNC and denoted by Pos. 1 and Pos. 3, and the third is located in the middle of CNC and denoted by Pos. 2. The geometric dimensions and the boundary conditions are as same as un-defected cases. The results are illustrated in Figure 8. As it is obvious in this figure, defect decreased the Young's modulus of CNCs. The most decrease is related to the defect that is located in position 2. This means that defects which are almost further than boundaries, have more influence on decreasing of Young's modulus.

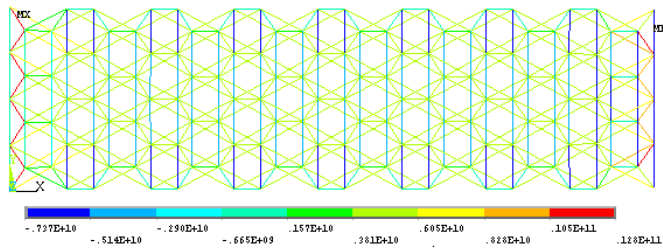


Figure 3. Generated axial stress in graphene sheet

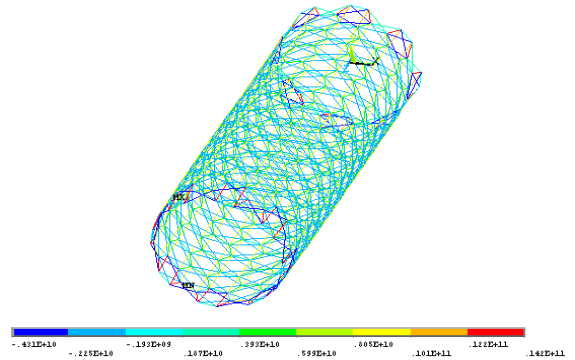
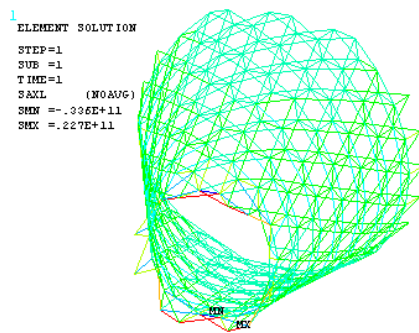
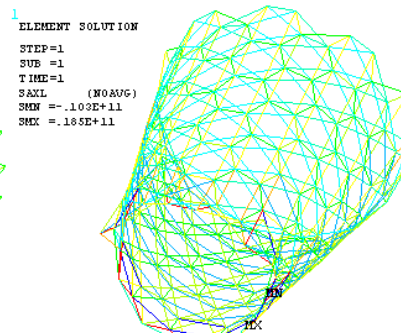


Figure 4. Generated axial stress in CNT

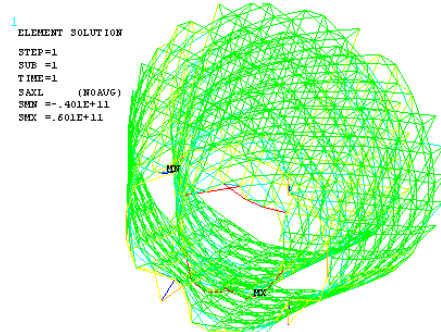


Apex angle = 38.9°

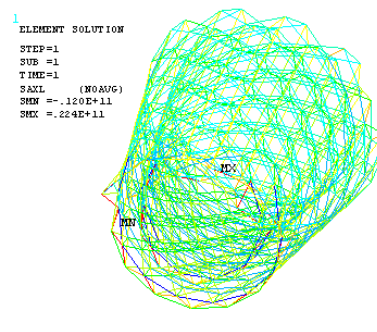


Apex angle = 19.2°

Figure 5. Generated axial stress in two SWCNCs



Apex angle = 38.9°



Apex angle = 19.2°

Figure 6. Generated axial stress in two DWCNCs

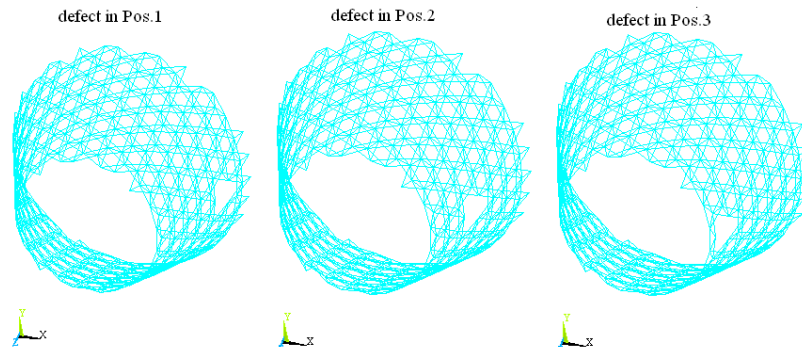


Figure 7. Defect and its position in CNC

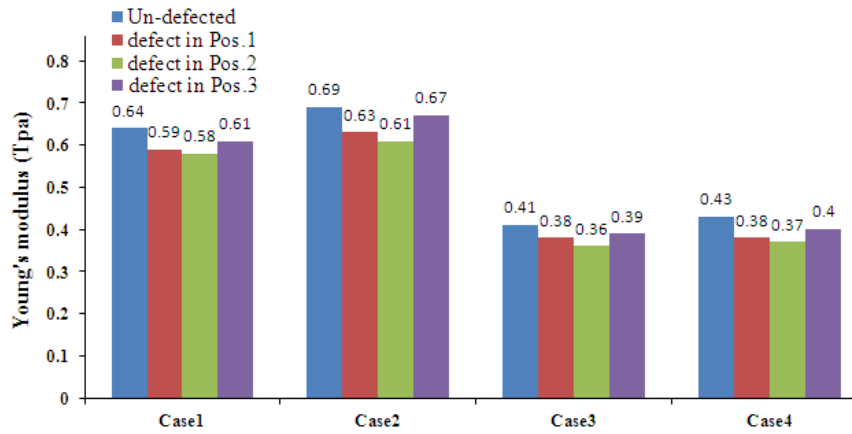


Figure 8. Effect of defect on Young's modulus of CNC

TABLE 1. Obtained Young's Modulus of Graphene Sheet

Sheet dimensions		Young's modulus (Tpa)	
Length(nm)	Width(nm)	Present work	Ref. [28]
2.84	0.74	0.958	0.995
3.13	0.98	0.993	1.002
4.83	1.97	1.010	1.021
9.85	1.97	1.018	1.024

TABLE 2. Obtained Young's Modulus of CNTs

CNT type	Diameter (nm)	Length (nm)	Young's modulus(Tpa)
(7,7)	0.949	≈ 5	0.964
(8,8)	1.085	≈ 2	1.023
(9,0)	0.704	≈ 8	0.960
(22,0)	1.72	≈ 10	1.031

TABLE 3. The Properties of Selected SWCNCs

CNC type	Apex angle	smallest radius(Å)	Largest radius(Å)	Number of nodes	Number of bond elements	Number of non-bond elements
Case1	19.2°	4.10	6.52	195	276	522
Case2	19.2°	5.46	7.82	266	380	704
Case3	38.9°	4.06	8.99	280	394	748
Case4	38.9°	7.16	11.9	396	557	1000

TABLE 4. The Longitudinal Stiffness and Young's Modulus of CNCs

CNC type	Stiffness (Nm <sup>-1</sup> )	Young's modulus(Tpa)
Case 1	512	0.643
Case 2	703	0.696
Case 3	394	0.419
Case 4	620	0.436
DWCNC1	1204	0.671
DWCNC2	1020	0.429

## 5. CONCLUSION

In this paper, Young's modulus of SWCNCs and DWCNCs is obtained using finite element method. For modeling of CNCs, two elastic rods are used for representing the bond stretching and the bond angle variation between carbon atoms. For the CNCs, the value of Young's modulus is obtained in the range of 0.4Tpa to 0.7Tpa. Results showed that an increase in the apex angle can decrease the modulus. Furthermore, in CNC with a fixed length, an increase in the diameter can lead to increment of modulus. In DWCNCs, the value of this elastic constant lies between the values of each layer. Also, defects decrease the Young's modulus and this decrement is influenced by the position of defects in CNC.

## 6. REFERENCES

- Wei, J., Liew, K.M. and He, X., "Mechanical properties of carbon nanocones", *Applied Physics Letters*, Vol. 91, No. 26, (2007), 261-270.
- Berber, B. and Kwon, Y.K.a.T., D., "Electronic and structural properties of carbon nanocones", *Physical Review B*, Vol. 62, (2000), 2291-2294.
- Yang, N., Zhang, G. and Li, B., "Carbon nanocone: A promising thermal rectifier", *Applied Physics Letters*, Vol. 93, No. 24, (2008), 243-111.
- Afzali, J. and Alemipour, Z., and Hesam, M., "High resolution image with multi wall carbon nanotube atomic force microscopy tip", *International Journal of Engineering*, Vol. 26, (2013), 671-676.
- Chen, I.-C., Chen, L.-H., Ye, X.-R., Daraio, C., Jin, S., Orme, C.A., Quist, A. and Lal, R., "Extremely sharp carbon nanocone probes for atomic force microscopy imaging", *Applied Physics Letters*, Vol. 88, No. 15, (2006), 153-160.
- Chen, I.-C., Chen, L.-H., Gapin, A., Jin, S., Yuan, L. and Liou, S.-H., "Iron-platinum-coated carbon nanocone probes on tipless cantilevers for high resolution magnetic force imaging", *Nanotechnology*, Vol. 19, No. 7, (2008), 75-100.
- Hsieh, J.-Y., Chen, C., Chen, J.-L., Chen, C.-I. and Hwang, C.-C., "The nanoindentation of a copper substrate by single-walled carbon nanocone tips: A molecular dynamics study", *Nanotechnology*, Vol. 20, No. 9, (2009), 96-105.
- Yu, S.-S. and Zheng, W.-T., "Effect of n/b doping on the electronic and field emission properties for carbon nanotubes, carbon nanocones, and graphene nanoribbons", *Nanoscale*, Vol. 2, No. 7, (2010), 1069-1082.
- Ge, M. and Sattler, K., "Observation of fullerene cones", *Chemical Physics Letters*, Vol. 220, No. 3, (1994), 192-196.
- Fereidoon, A., Mottahedin, L. and Latibari, S.T., "Investigation of fracture toughness parameters of epoxy nanocomposites for different crack angles", (2012).
- Chaboki Khiabani, A., Sadrnejad, S. and Yahyaieii, M., "Stress transfer modeling in cnt reinforced composites using continuum mechanics", Vol., (2008).
- Tsai, P.-C. and Fang, T.-H., "A molecular dynamics study of the nucleation, thermal stability and nanomechanics of carbon nanocones", *Nanotechnology*, Vol. 18, No. 10, (2007), 105-110.
- Liew, K., Wei, J. and He, X., "Carbon nanocones under compression: Buckling and post-buckling behaviors", *Physical Review B*, Vol. 75, No. 19, (2007), 195-204.
- Liao, M.-L., Cheng, C.-H. and Lin, Y.-P., "Tensile and compressive behaviors of open-tip carbon nanocones under axial strains", *Journal of Materials Research*, Vol. 26, No. 13, (2011), 1577-1584.
- Kumar, D., Verma, V., Bhatti, H. and Dharamvir, K., "Elastic moduli of carbon nanohorns", *Journal of Nanomaterials*, Vol. 2011, (2011), 13-20.
- Firouz-Abadi, R., Fotouhi, M. and Haddadpour, H., "Free vibration analysis of nanocones using a nonlocal continuum model", *Physics Letters A*, Vol. 375, No. 41, (2011), 3593-3598.
- Seyyed Fakhrabadi, M.M., Khani, N. and Pedrammehr, S., "Vibrational analysis of single-walled carbon nanocones using molecular mechanics approach", *Physica E: Low-dimensional Systems and Nanostructures*, Vol. 44, No. 7, (2012), 1162-1168.
- Chang, T. and Gao, H., "Size-dependent elastic properties of a single-walled carbon nanotube via a molecular mechanics model", *Journal of the Mechanics and Physics of Solids*, Vol. 51, No. 6, (2003), 1059-1074.
- Nasdala, L. and Ernst, G., "Development of a 4-node finite element for the computation of nano-structured materials", *Computational Materials Science*, Vol. 33, No. 4, (2005), 443-458.
- Leung, A., Guo, X., He, X. and Kitipornchai, S., "A continuum model for zigzag single-walled carbon nanotubes", *Applied Physics Letters*, Vol. 86, No. 8, (2005), 83-110.
- Nahas, M.N. and Abd-Rabou, M., "Finite element modeling of carbon nanotubes", *Submitted to Computational Materials Science*, (2010).
- Rafiee, R. H., M., "Young's modulus prediction of carbon nanotubes using full nonlinear interatomic potentials", *16th International Conference on Composite Structures, Porto*, (2011).
- Terrones, H., Hayashi, T., Munoz-Navia, M., Terrones, M., Kim, Y., Grobert, N., Kamalakaran, R., Dorantes-Davila, J., Escudero, R. and Dresselhaus, M., "Graphitic cones in palladium catalysed carbon nanofibres", *Chemical physics letters*, Vol. 343, No. 3, (2001), 241-250.
- Tsakadze, Z., Levchenko, I., Ostrikov, K. and Xu, S., "Plasma-assisted self-organized growth of uniform carbon nanocone arrays", *Carbon*, Vol. 45, No. 10, (2007), 2022-2030.
- Ansari, R., Alisafaei, F., Alipour, A. and Mahmoudinezhad, E., "On the van der waals interaction of carbon nanocones", *Journal of Physics and Chemistry of Solids*, Vol. 73, No. 6, (2012), 751-756.
- Belytschko, T., Xiao, S., Schatz, G. and Ruoff, R., "Atomistic simulations of nanotube fracture", *Physical Review B*, Vol. 65, No. 23, (2002), 235-250.
- Denn, M.M., "Optimization by variational methods", (1969).
- Li, C. and Chou, T.-W., "A structural mechanics approach for the analysis of carbon nanotubes", *International Journal of Solids and Structures*, Vol. 40, No. 10, (2003), 2487-2499.
- Lei, X., Natsuki, T., Shi, J. and Ni, Q.-Q., "Analysis of carbon nanotubes on the mechanical properties at atomic scale", *Journal of Nanomaterials*, Vol. 2011, (2011), 1-10.
- Parvaneh, V. and Shariati, M., "Effect of defects and loading on prediction of young's modulus of swcnets", *Acta Mechanica*, Vol. 216, No. 1-4, (2011), 281-289.
- Sadrnejad, S.A. and Chaboki, A.a.Y., M., "Inelastic continuum modeling of carbon nanotubes behavior using finite element method", *International Journal of Engineering Transactions A*, Vol. 20, (2007), 129-135.

## APPENDIX

A multi walled nanocone with  $n$  layers is shown in Figure 9. It is assumed that all layers have the same apex angle ( $\alpha$ ). The left end is fully fixed while the other end is subjected to a stretching horizontal load. For an element with the length of  $dx$  which is located in position  $x$ , the relation between load ( $P$ ) and length variation ( $\Delta l$ ) can be written as follows:

$$\Delta l = \frac{P dx}{2p E \sum_{i=1}^n r x_i} \quad (14)$$

For a cone we have:

$$r x_i = r_{0_i} + x \tan(\alpha / 2) \quad (15)$$

by substituting above equation in Equation (14), the total length variation ( $\Delta L$ ) of MWCNC is obtained as follows:

$$\Delta L = \int_0^L \frac{P dx}{2p E \left( \sum_{i=1}^n r_{0_i} + x \tan(\alpha / 2) \right)} \quad (16)$$

So, the Young's modulus of the MWCNC in longitudinal direction is:

$$E = \frac{K}{2pm \tan(\alpha / 2)} \ln \left( 1 + \frac{nL \tan(\alpha / 2)}{\sum_{i=1}^n r_{0_i}} \right) \quad (17)$$

where,  $K$  is the stiffness of MWCNC and is equal to  $P/\Delta L$ .

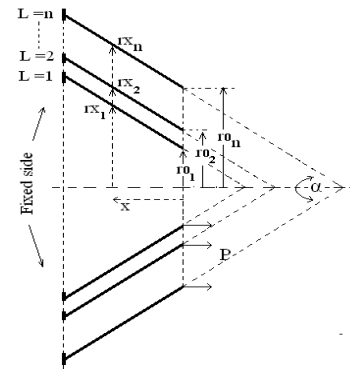


Figure 9. A multi walled nanocone which is subjected to a longitudinal direction

## Young's Modulus of Single and Double Walled Carbon Nanocones Using Finite Element Method

## TECHNICAL NOTE

M. Mohammadian<sup>a</sup>, Ab. Fereidoon<sup>b</sup>

<sup>a</sup>Department of Mechanical Engineering, University of Islamic Azad, Gorgan branch, Kordkuy center

<sup>b</sup> Faculty of Mechanical Engineering, University of Semnan

### PAPER INFO

چکیده

#### Paper history:

Received 08 November 2013

Received in revised form 27 February 2014

Accepted 22 May 2014

#### Keywords:

Carbon Nanocones  
Truss Model  
LINK8 Element  
ANSYS

در این مقاله یک مدل المان محدود سه بعدی از نانومخروط های کربنی ارائه شده و از آن جهت بدست آوردن مدول یانگ نانومخروط کربنی تک لایه و دولایه استفاده گردیده است. در این مدل نیروهای کششی و خمشی بین اتم های کربن با استفاده از المان های خرابا در نرم افزار انسیس شبیه سازی شده و سپس با اعمال کشش و بدست آوردن سختی نانومخروط و به کمک تئوری الاستیسیته، مدول یانگ محاسبه شده است. نتایج نشان داد در یک نانومخروط با طول ثابت، مدول با افزایش قطر افزایش می یابد، درحالی که با افزایش زاویه راس مخروط مقدار مدول کاهش می یابد. همچنین مدول یانگ نانومخروط دولایه کربنی بدست آمده بین مقادیر مدول لایه های آن قرار دارد. علاوه براین، اثر خرابی و موقعیت آن در مقدار مدول یانگ بررسی شده است.

oi:10.5829/idosi.ije.2014.27.09c.17